Fractional Spin Textures in the Frustrated Magnet $SrCr_{9p}Ga_{12-9p}O_{19}$

Arnab Sen,[1,2] Kedar Damle,[1] and Roderich Moessner[3]

[1]*Tata Institute of Fundamental Research, 1, Homi Bhabha Road, Mumbai 400005, India*
[2]*Department of Physics, Boston University, 590 Commonwealth Avenue, Boston, Massachusetts 02215, USA*
[3]*Max-Planck-Institut für Physik komplexer Systeme, 01187 Dresden, Germany*

(Received 26 July 2010; revised manuscript received 29 September 2010; published 23 March 2011)

We consider the archetypal frustrated antiferromagnet $SrCr_{9p}Ga_{12-9p}O_{19}$ in its well-known spin-liquid state, and demonstrate that a Cr^{3+} spin $S = 3/2$ ion in direct proximity to a pair of vacancies (in disordered $p < 1$ samples) is cloaked by a spatially extended spin texture that encodes the correlations of the parent spin liquid. In this spin-liquid regime, our analytic theory predicts that the combined object has a magnetic response identical to a classical spin of length $S/2 = 3/4$, which dominates over the small intrinsic susceptibility of the pure system. This fractional-spin texture leaves an unmistakable imprint on the measured ^{71}Ga nuclear magnetic resonance line shapes, which we compute using Monte Carlo simulations and compare with experimental data.

DOI: 10.1103/PhysRevLett.106.127203 PACS numbers: 75.10.Jm, 05.30.Jp, 71.27.+a

Quantum mechanics constrains the total electronic spin S of magnetic ions to integer or half-integer values. For an isolated ion with only spin angular momentum and Lande g-factor $g_L = 2$, this results in a magnetic moment of $\mu = 2\mu_B S$, and a susceptibility $(2\mu_B)^2 S(S+1)/3T$, which is approximated by $(2\mu_B)^2 S^2/3T$ when spins are treated as classical length-S vectors. Here, we demonstrate that certain vacancy configurations, in a class of corner-sharing networks made up of such spin-S ions coupled antiferromagnetically, give rise to an extended object with classical susceptibility $(2\mu_B)^2(S/2)^2/3T$. This corresponds to a fractional moment of $\mu/2$ and represents an instance of fractionalization [1] yielding a fractional "effective spin" $S/2$ in a classical setting.

This striking prediction is of direct relevance to measurements on $SrCr_{9p}Ga_{12-9p}O_{19}$ (SCGO), a remarkable magnetic material [2–4] which, for a range of density $x \equiv 1 - p$ of vacancies in its corner-sharing network [Fig. 1] of antiferromagnetically coupled Cr^{3+} $S = 3/2$ moments, does not show any signs of magnetic ordering [5] even at extremely low temperatures $T \sim \Theta_{CW}/100$, where $\Theta_{CW} \approx 500$ K is the so-called Curie-Weiss temperature at which mean-field theory predicts magnetic ordering of the Cr^{3+} spins. Two key features of this broad regime of "spin-liquid" behavior in SCGO are of particular interest here. The first is the presence of a paramagnetic "Curie tail" in the low temperature uniform susceptibility of these compounds, well modeled by a defect contribution $\chi_{\text{defect}} = C_d/T$ that dominates over the intrinsic susceptibility $\chi_{\text{intrinsic}} \approx C_1/(T + \Theta_{CW})$ for $T \ll \Theta_{CW}$; the Curie constant C_d in this "two-population" phenomenology was associated with a population of paramagnetic objects dubbed "orphan spins" [6]. The second is the apparently symmetric nuclear magnetic resonance (NMR) line broadening ΔH that scales as $\Delta H \propto x/T$ for not-too-low x and T; this was in turn interpreted phenomenologically as a signature of a short-ranged, oscillating spin density profile or "spin texture" induced by some lattice defects [7].

Our work builds on two previous theoretical results: The first, obtained using a "single-unit approximation"[8], predicts that "defective" simplices (corner-sharing units), in which all but one spin has been substituted for with nonmagnetic impurities, must give rise to Curie tails in the low temperature susceptibility of isotropic classical spin-S antiferromagnets on corner-sharing lattices such as SCGO. The second uses classical energy minimization considerations at $T = 0$ to argue that an infinitesimal magnetic field applied to such a system with a single defective simplex should induce a $T = 0$ spin-texture with total spin projection $S/2$

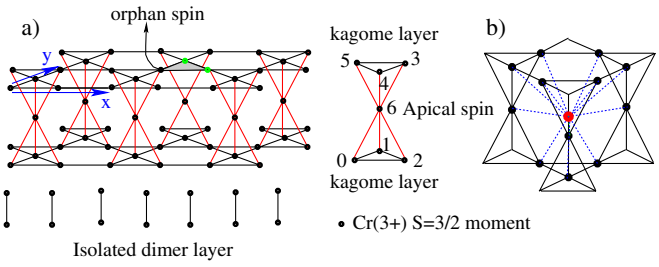

FIG. 1 (color online). (a) The Cr atoms in SCGO form a lattice of kagome bilayers separated from each other by a layer of isolated dimers consisting of pairs of Cr atoms. Each kagome bilayer is a corner-sharing arrangement of tetrahedra and triangles made up of two kagome lattices coupled to each other through "apical" sites shared between up-pointing and down-pointing tetrahedra. Links between near-neighbor sites in each bilayer represent a Heisenberg exchange coupling $J = 80$ K between neighboring Cr^{3+} spins, while links in the isolated dimer layer represent a Heisenberg exchange coupling $J' = 216$ K between the two Cr^{3+} ions that constitute each pair. Two vacancies in a triangle [(green) circles] leave behind an orphan spin. (b) The 12 Cr^{3+} sites (black) that are hyperfine coupled to a given Ga ($4f$) site (red) in the SCGO lattice.

in the direction of the field [9]. This suggests that the phenomenological orphan spins [6] and oscillating spin textures [7] invoked earlier are related to the presence of such defective simplices, with the lone spins on such defective simplices providing a microscopic basis for the phenomenological orphan spin population of Ref. [6].

Although this orphan-texture complex (comprising this orphan spin on a defective simplex and its surrounding spin texture) is thus implicated in some of the most intriguing experimental observations on SCGO, a fundamental understanding of it has been lacking. Here, we develop a quantitatively accurate analytical theory that provides a full characterization of this orphan-texture complex by accounting for both entropic and energetic effects in the spin-liquid regime of low temperatures ($\bar{T} \equiv k_B T/JS^2 \ll 1$) and low magnetic field h ($\bar{h} \equiv g_L \mu_B h/JS \ll 1$), but arbitrary $\bar{h}/\bar{T}$. In this regime, we find that the orphan spin magnetization is equal to the magnetization of a spin S in a field $h/2$. This is accompanied by an extended spin texture, which is scale-free at $T = 0$ but acquires a finite extent as T is increased. We determine the intricate pattern of spin correlations in the texture and demonstrate that its net magnetization cancels off half of the orphan spin's moment, thus giving rise to an orphan-texture complex that behaves as a classical spin $S/2$ in field h, with a susceptibility given within the classical approximation by

$$\chi_{S/2}(T) = (g_L \mu_B)^2 (S/2)^2 / 3k_B T.$$

In remarkable correspondence with experiment [7], we find that these extended, fractional-spin orphan-texture complexes show up prominently in SCGO at not-too-low $x = 1 - p$ as a large, nearly symmetric low temperature broadening $\Delta H \propto x/T$ of our predictions for the ^{71}Ga($4f$) NMR line [7] associated with Ga nuclei at the so-called ($4f$) crystallographic position in the SCGO lattice [Fig. 1]. We therefore focus below on this particular case, although our analytical low temperature, low-field results are expected to apply more generally to orphan-texture complexes surrounding isolated defective simplices in the spin-liquid regime of classical Heisenberg antiferromagnets on the hyper-kagome and pyrochlore lattices as well.

Within the classical approximation, SCGO is described by the energy function

$$\mathcal{H} = \frac{J}{2} \sum_{\boxtimes} \Big(\sum_{i \in \boxtimes} \vec{S}_i - \frac{g_L \mu_B \vec{h}}{2J} \Big)^2 + \frac{J}{2} \sum_{\Delta} \Big(\sum_{i \in \Delta} \vec{S}_i - \frac{g_L \mu_B \vec{h}}{2J} \Big)^2$$

where $\vec{S}_i$ are classical length-S spins ($S = 3/2$ for SCGO) with saturation moment $g_L S$ in units of the Bohr magneton μ_B ($g_L = 2$ in SCGO), J is the nearest-neighbor Heisenberg exchange coupling ($J \simeq 80$ K for SCGO [7]), and $\vec{h}$ is the external field. $\boxtimes$ refers to the tetrahedra that consisting of a triangle in a kagome layer attached to an apical spin in the triangular layer [Fig. 1], while Δ refers to those triangles in the kagome layer which are not associated with an apical spin.

Here, we model the pure $p = 1$ system in terms of an effective free energy functional $\mathcal{F}$ that incorporates the energetics of the antiferromagnetic interactions J on an equal footing with entropic effects of thermal fluctuations

$$\mathcal{F} = \mathcal{H}(\{\vec{\phi}_i\}) + \frac{T}{2} \sum_i \rho_i \vec{\phi}_i^2.$$

The unconstrained effective field $\vec{\phi}_i$ serves as a surrogate for the microscopic fixed-length spin variables $\vec{S}_i$, with the statistical weight of a field configuration $\{\vec{\phi}_i\}$ being proportional to $\exp(-\mathcal{F}/T)$. $\mathcal{H}(\{\vec{\phi}_i\})$ is the classical Hamiltonian of the system now written in terms of $\vec{\phi}_i$, and the phenomenological stiffness constants ρ_i are fixed by requiring that the mean length of $\vec{\phi}_i$ equal S within the effective theory: $\langle \vec{\phi}_i^2 \rangle_{\mathcal{F}} = S^2$ [10]. For a background to this approach for pure systems, see the review by Henley [11].

To incorporate disorder effects in diluted $p < 1$ samples, we assume that the stiffness constants do not change significantly from their pure values, but extend the effective theory in two important ways: First, we model vacancies in the lattice by setting $\vec{\phi}_i$ to zero on vacancy sites; second, and more crucially, as the fixed-length nature of an orphan spin on a defective simplex is expected to play a central role, we retain it as a microscopic length-S spin and do not introduce an effective field variable at such sites.

We now use this effective theory to analyze the SCGO magnet with a single defective triangle, i.e., two vacancies on one triangle of the SCGO lattice [Fig. 1]. In this case, the effective theory reduces to a length-S orphan spin $S\vec{n}$ ($\vec{n}^2 = 1$) coupled to a constrained Gaussian theory for $\vec{\phi}_i$ (with constraints $\vec{\phi}_i = 0$ at the two vacancy sites). Focusing first on the orphan spin $S\vec{n}$ in this defective triangle by integrating out the $\vec{\phi}$ fields, we find [10] that the exchange field from the surrounding spin-liquid "screens" exactly half the external magnetic field on the orphan spin in the low temperature, low-field spin-liquid regime, yielding a spin S variable that "sees" a magnetic field $h/2$, and, therefore, develops a polarization equal to that of a free classical spin S in a field $h/2$. This striking prediction is fully confirmed by Monte Carlo studies [10] of the classical SCGO magnet with one defective triangle [see Fig. 2(a)], which also reveal that this prediction is surprisingly robust, remaining accurate for temperatures as high as $T \sim 0.1JS^2$ for this example.

Next, we turn to a detailed description of the extended spin texture that cloaks this orphan spin in the spin-liquid regime. In addition to the uniform external field $\vec{h} = h\hat{z}$ that acts on all the $\vec{\phi}_i$ in the constrained Gaussian action, this orphan spin polarization also gives rise to a local exchange field that acts in the $\hat{z}$ direction on $\vec{\phi}_i$ at the two undiluted sites adjacent to the orphan spin.

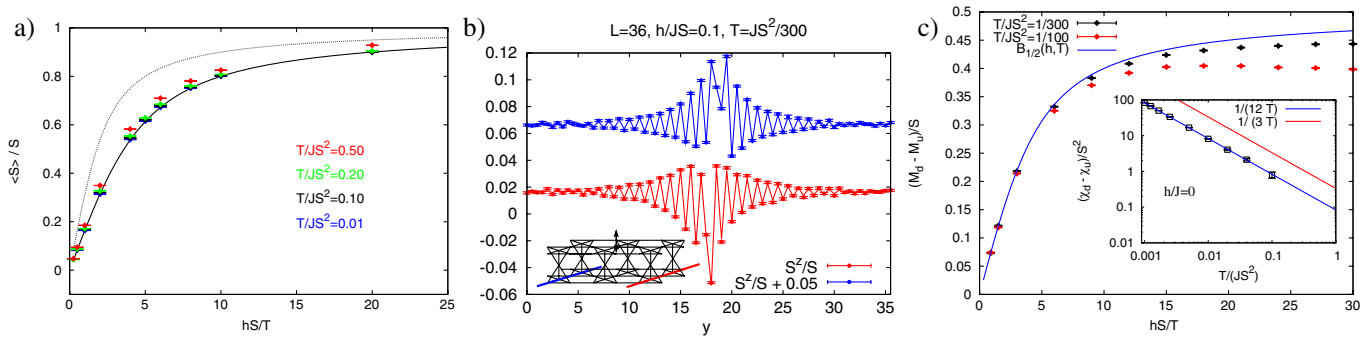

FIG. 2 (color online). (a) In the spin-liquid regime, the orphan spin in field h develops magnetization (symbols) that matches $B_S(h/2, T)$, the magnetization of a spin S in field $h/2$ (full line). The dotted curve is the magnetization for an isolated spin S in field h. (b) The orphan induced spin texture shown along two cuts on the lattice. Numerical data are shown as points with error bars and the effective theory result as lines. The spin texture shown at the top (bottom) of the main plot is along the cut shown on the left (right) of the orphan spin (arrow) in the inset. The orphan spin is denoted by an arrow in the inset. (c) The impurity magnetization (defined in text) of a single orphan-texture complex (symbols) compared with $B_{S/2}(h, T)$ (solid curve), the magnetization curve of a classical spin $S/2$ in the spin-liquid regime. Note the much faster convergence of numerical data to $B_{S/2}(h, T)$ in the linear (small hS/T) part of the magnetization curve. Inset: The corresponding impurity susceptibility (defined in text) matches the susceptibility of a free classical spin $S/2$ up to temperatures $T \sim 0.1JS^2$.

The extended spin texture surrounding the orphan spin is modeled within the effective theory by calculating the response $\langle \phi_i^z \rangle_{\mathcal{F}}$ to these fields [10]. At $T = 0$, the computed texture's envelope decays as $1/|\vec{r}|$ away from the orphan spin, while the overall scale is set by the orphan spin's saturation magnetization. At finite-T and small fields in the spin-liquid regime, the power law envelope is cut off by a thermally introduced finite correlation length $\xi \sim 1/\sqrt{T}$, endowing it with an effective size $\xi^d \sim 1/T^{d/2}$ in d dimensions; in our $d = 2$ example, this gives a spatial size $\sim 1/T$ scaling identically with the overall magnetization scale of the texture, which is set by the orphan spin's susceptibility $\sim 1/T$. These predictions are compared with Monte Carlo simulation [10] results in Fig. 2(b) for the case of a single defective triangle in SCGO, and the agreement is remarkably good.

Although the computed texture decays slowly (as $1/|\vec{r}|$ at $T = 0$), its oscillations conspire to reduce its net moment so that it cancels out precisely half of the orphan spin's moment, endowing the orphan-texture complex with a net "impurity magnetization" (excess magnetization over and above that of a pure system in the same external field) equal to the magnetization of a classical spin $S/2$ in field h. The corresponding "impurity susceptibility" χ_{imp} arising from a single orphan-texture complex is $(g_L \mu_B S/2)^2/3k_B T$—a Curie tail dominating the low-T response. For the case of a single defective triangle in SCGO, our Monte Carlo simulations validate this striking prediction up to surprisingly high temperatures of order $T \sim 0.1JS^2$ [Fig. 2(c)].

Fortunately, this novel physics leaves its imprint on the Ga(4f) NMR line, which is a sensitive probe of the distribution of the 12 Cr spin polarizations that are hyperfine coupled to each Ga ($4f$) nucleus in SCGO [Fig. 1(b)]. We calculate this distribution [10] in diluted SCGO lattices with vacancy density $x = 1 - p$ (which we model by assigning an uncorrelated site dilution probability of x), using the experimentally known values [7] of these hyperfine couplings, and Monte Carlo simulations [10] of the original spin system to fully account for the physics of a nonzero density of orphan spins in order to obtain quantitatively accurate results.

As is clear from the example at $x = 0.2$ shown in Fig. 3(a), this calculation predicts a line that is broad and appears symmetric, reflecting the fact that the spin textures are staggered and involve a very large number of spins, making it difficult to discern the $O(1)$ net moment of each texture that endows the line with a slight bias towards lower magnetic fields.

In Fig. 3(c), we show the temperature and x dependence of the width of our predicted lines for not-too-small values of x and T, of greatest relevance to experiments. As the line shape is not well-approximated by a Gaussian, we do not fit the line to a Gaussian, but rather use the definition $\Delta H \equiv 2\sqrt{2\ln(2)}(\langle H^2 \rangle - \langle H \rangle^2)^{1/2}$ which reduces to the standard value for a Gaussian line but provides an unbiased measure of the width in more general cases. As is clear from Fig. 3(c), the theoretical predictions for ΔH have the expected "Curie tail" $\Delta H \sim \mathcal{A}(x)/T$ at low temperature. For uncorrelated site dilution, the coefficient $\mathcal{A}$ is expected to scale as x^2 for asymptotically small x; however, for not-too-small x relevant to experiment, we find that $\mathcal{A}(x)$ can be fit well by an approximately linear x dependence $\mathcal{A}(x) \sim x$.

Thus, our theory reproduces the broad, apparently symmetric lines seen in experiments, with broadening scaling as $\Delta H \sim x/T$ for not-too-low x and T. Although these experimental facts are fully reproduced, we caution that our results do not provide a fully quantitative explanation of the NMR data: As is clear from Fig. 3(b), our minimal disorder model consisting of independent vacancies of the

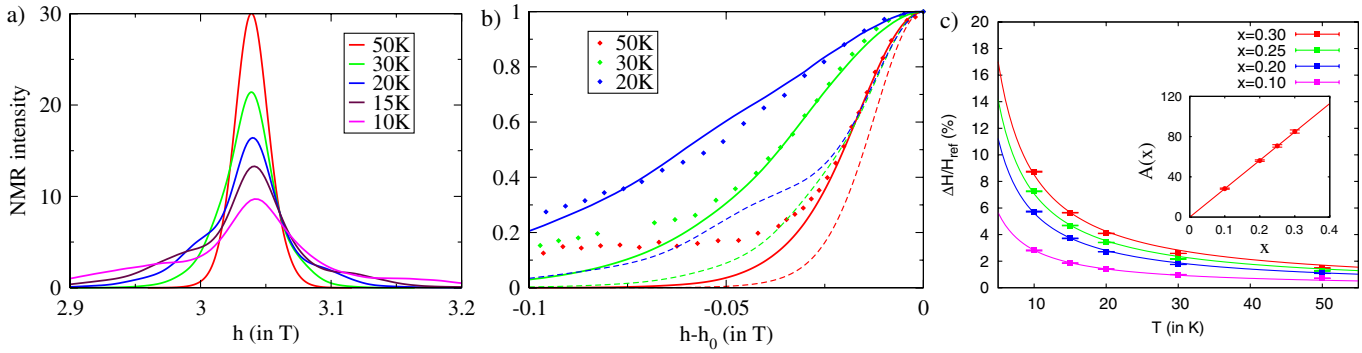

FIG. 3 (color online). (a) ^{71}Ga($4f$) "field-scan" NMR lines predicted [10] within the minimal disorder model of uncorrelated dilution at vacancy density $x = 0.2$. (b) Experimental results of Ref. [7] for field-scan ^{71}Ga($4f$) NMR lines (dots) at dilution $x = 0.19$ compared to theoretical predictions of the minimal disorder model (with y axis rescaled and x axis offset appropriately for easy comparison of linewidths and shapes of all curves) at vacancy density $x = 0.2$ (dashed curves) and $x = 0.3$ (full curves). Only the low-field side of the experimental line is compared with theory, as the high-field side is known to be contaminated by the presence of a satellite peak arising from nonstoichiometric (impurity) ^{71}Ga nuclei located at three different Cr sites in the SCGO lattice [7]. (c) Temperature and x dependence of the width ΔH of the theoretically predicted field-scan ^{71}Ga($4f$) NMR lines, normalized by a reference field $H_{\rm ref} = 3.12$ T. Solid curves in the main plot are fits of ΔH to $\mathcal{A}(x)/T$ over the experimentally relevant temperature range, and inset shows the approximately linear x dependence of the corresponding best-fit values of $\mathcal{A}(x)$.

nominal experimental vacancy density significantly underestimates the absolute scale of the linewidth ΔH. Since isolated vacancies lead to no oscillating spin textures scaling as $1/T$ [10], this discrepancy clearly demonstrates that the density of orphan spins in the experimental samples is significantly higher than that expected from uncorrelated Ga substitution of the Cr lattice. The most frugal resolution is perhaps that the Ga substitution in the Cr kagome layer may be correlated. Additionally, and perhaps more realistically, other sources of disorder, for instance strain-induced bond randomness, could also affect the effective density of "orphan spins". Unfortunately, measurements [6] of the impurity Curie constant C_d probably cannot shed light on this, as uniform susceptibility measurements also pick up, apart from the signal due to Kagome layer orphan spin textures, a much larger "background" contribution from free Cr spins created when Ga impurities substitute for Cr in the isolated dimer layer [Fig. 1].

In conclusion, these disorder-induced orphan-texture complexes in SCGO embody several central themes of modern condensed matter physics: The emergence of new types of extended degrees of freedom, and their rich physics at finite density, is a common strand that runs through diverse examples [12] such as Skyrmion lattices in spinor condensates [13], itinerant [14] and quantum Hall magnets [15,16], and spin textures in topological phases of matter [17]. Moreover, the fact that our textures give rise to a relatively strong magnetic response—their staggered $1/r^{d-1}$ magnetization profile is parametrically stronger than the intrinsic $1/r^d$ spin correlations of the parent spin-liquid—shows that, like in the case of defects evidencing the d-wave nature of the order parameters in the cuprates, imperfections are among the best and most direct probes of exotic correlated states of matter.

The authors thank P. Mendels for providing the original NMR data [Fig. 3(b)] and gratefully acknowledge useful discussions with F. Bert, D. Dhar, C. Henley, P. Mendels, P. Schiffer, and A. Zorko, funding from DST SR/S2/RJN-25/2006, financial support for collaborative visits from the Fell Fund (Oxford), the ICTS TIFR (Mumbai), ARCUS (Orsay), and MPIPKS (Dresden), as well as computational resources at TIFR.

[1] R. Rajaraman, *Quantum (Un)speakables* edited by R. A. Bertlemann and A. Zeilinger (Springer-Verlag, Berlin2002), pp. 383–399.
[2] X. Obradors *et al.*, Solid State Commun. **65**, 189 (1988).
[3] B. Martinez, A. Labarta, R. Rodriguez-Sola, and X. Obradors, Phys. Rev. B **50**, 15779 (1994).
[4] A. P. Ramirez, G. P. Espinosa, and A. S. Cooper, Phys. Rev. Lett. **64**, 2070 (1990).
[5] Y. J. Uemura *et al.*, Phys. Rev. Lett. **73**, 3306 (1994).
[6] P. Schiffer and I. Daruka, Phys. Rev. B **56**, 13712 (1997).
[7] L. Limot *et al.*, Phys. Rev. B **65**, 144447 (2002).
[8] R. Moessner and A. J. Berlinsky, Phys. Rev. Lett. **83**, 3293 (1999).
[9] C. L. Henley, Can. J. Phys. **79**, 1307 (2001).
[10] See supplementary material at http://link.aps.org/supplemental/10.1103/PhysRevLett.106.127203.
[11] C. L. Henley, arXiv:0912.4531 (unpublished).
[12] C. Day, Phys. Today **62**, 4, 12 (2009).
[13] R. W. Cherng, Ph.D. thesis, Harvard University, 2009.
[14] S. Mühlbauer *et al.*, Science **323**, 915 (2009).
[15] S. L. Sondhi, A. Karhelde, S. A. Kivelson, and E. H. Rezayi, Phys. Rev. B **47**, 16419 (1993).
[16] G. Gervais *et al.*, Phys. Rev. Lett. **94**, 196803 (2005).
[17] D. Hsieh *et al.*, Science **323**, 919 (2009).